

# Low Temperature Solid-State Extrusion of Recycled Poly(ethylene terephthalate) Bottle Scraps

Weihong Guo, Xianwen Tang, Guorong Yin, Yuanji Gao, Chifei Wu

*Polymer Alloy Laboratory, School of Materials Science and Engineering, East China University of Science and Technology, Shanghai 200237, People's Republic of China*

Received 2 July 2005; accepted 31 December 2005

DOI 10.1002/app.24101

Published online in Wiley InterScience (www.interscience.wiley.com).

**ABSTRACT:** The processing of poly(ethylene terephthalate) (PET) involves thermal and hydrolytic degradation of the polymer chain, which reduces not only the intrinsic viscosity and molecular weight, but also the mechanical properties of recycled materials. A novel PET/bisphenol A polycarbonate/styrene-ethylene-butylene-styrene alloy based on recycled PET scraps is prepared by low temperature solid-state extrusion. Hydrolysis and thermal degradation of PET can be greatly reduced by low temperature solid-state extrusion because the extrusion temperature is between the glass-transition temperature and cold-crystallization

temperature of PET. Modification of recycled PET by low temperature solid-state extrusion is an interesting method; it not only provides an easy method to recycle PET scraps by blend processing, but it can also form novel structures such as orientation, crystallization, and networks in the alloy. © 2006 Wiley Periodicals, Inc. *J Appl Polym Sci* 102: 2692–2699, 2006

**Key words:** low temperature solid-state processing; recycled poly(ethylene terephthalate); network; crystallization; degradation

## INTRODUCTION

Presently the large amount of disposable bottles makes it imperative to search for recycling or reuse methods of these materials, because they are not biodegradable. According to Selke,<sup>1</sup> the total amount of plastics in the U.S. municipal solid waste stream is around 10%; 44% of this amount is from containers and packaging. A large quantity of these containers comes from soft drink bottles. The fact that some states in the United States are concerned with recycling (e.g., Michigan, where the recycling rate is close to 100%) proves the potential for recycling plastic waste. One possible solution for the municipality plastic waste problem is the recycling procedure. Plastic waste management can be done by three different approaches. The first one is the mechanical recycling approach, which is a technique similar to procedures used to recover materials suitable for second use. The second one is known as energy recovery, which can be performed in two distinct ways. The first way is incineration where the hydrocarbon polymers replace fossil fuels, and the second way is pyrolysis or hydrogenation of low molecular weight hydrocarbons for use either as portable fuels or as polymer feedstock. A third approach is biological recycling.

This approach takes advantage of polymer biodegradation, which is highly dependent on the polymer type and environmental conditions. However, this type of recycling most often involves not only high costs and complex procedures but also potential damage to the environment.<sup>2–10</sup>

Because chemical processing is often costly and sometimes aggressive to the environment, a possible solution is the recycling of such materials by low temperature processing techniques.<sup>11–17</sup> This article takes into consideration the recycling of postconsumer plastic bottles by low temperature solid-state extrusion, especially the ones made of poly(ethylene terephthalate) (PET), and their use as composite materials for engineering plastics. PET recycling is currently in a growing stage of development because this polymer is widely used in the manufacture of fibers, beverage bottles, and photographic supports. The thermal and hydrolytic degradation of recycled PET caused by the simultaneous presence of retained moisture, which comes from the shape of particles and contaminants, generates problems associated with the loss of molecular weight, which leads to a decrease in the intrinsic viscosity. The decrease in these two parameters affects the mechanical properties of recycled materials. The reduction in the chain length of PET caused by degradation of chain scission can be compensated for by the use of low temperature solid-state extrusion together with the use of a chain extender. To be able to evaluate the new composite performance, tests were carried out to measure the mechanical properties. The microstructures were tested and analyzed.

Correspondence to: C. Wu (guoweihong@ecust.edu.cn).

Contract grant sponsor: Natural Science Foundation of China; contract grant number: 20574019.

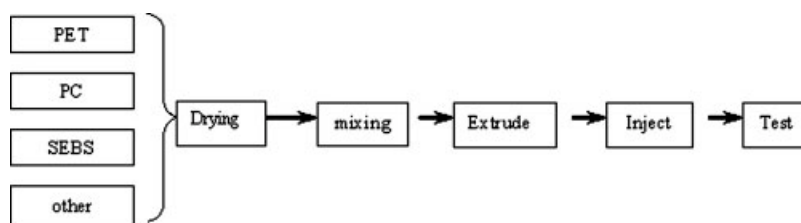


Figure 1 A sketch for processing.

## EXPERIMENTAL

### Materials and equipment

Virgin PET supplied by Zijang Bottle Ltd. (Shanghai, China) was a bottle-grade material with an intrinsic viscosity of 0.80 dL/g. Scraps of recycled PET with an intrinsic viscosity of 0.71 dL/g came from Zijang Bottle Ltd. Polycarbonate (PC) and styrene-ethylene-butylene-styrene (SEBS) were supplied by Teijin Ltd.

The twin-screw extruder used in the study was a TSE-35A from Nanjin Ruiya Polymer Machine Ltd. The injector was a QS-100T from Shanghai Quansheng Polymer Machine Ltd. The drying equipment was an MCE from Shanghai Qixin Machine Ltd.

### Processing

Pellets of virgin PET, scraps of PET, and PC were dried under a vacuum for 10 h at 120°C. After drying, PET, PC, and SEBS were blended with the twin-screw extruder. The granular blends after extrusion were injected to gain the specimen with an injector at 240°C. Chain extender was introduced before extruding with the polymer in the preheated batch mixer at 60 rpm for 3 min at 100°C. The processing sketch is shown in Figure 1.

The relationship between the glass-transition temperature ( $T_g$ ) and the components of the PET/PC alloy was tested by Zeng et al.<sup>18</sup> The blends have two  $T_g$  values when the PET content is higher than 60 and have only one  $T_g$  value when the PET content is less than 60. The  $T_g$  for PC is about 150°C and that for PET is approximately 80°C. They also performed dynamic mechanical analysis tests to prove the result that PET/PC blend is semicompatible. When the PC/PET ratio

was 75/25, the blend had good mechanical properties such as impact strength and elongation at break. Thus, the ratio of PET, PC, and SEBS was set to 60 : 20 : 20 in this research and testing.

### Characterization

Mechanical properties tests were conducted with a WSM-20KN mechanical properties testing machine produced by Chang Chun Mechanical Properties Testing Machine Ltd. Differential scanning calorimetry (DSC) was performed on a NETZSCH DSC PC 200. The heating rate was 10°C/min in N<sub>2</sub>. The  $T_g$  was determined by the temperature diagrams as the temperature corresponding to the upper inflection point or maximum of the curve. The melting point ( $T_m$ ) and crystallization temperatures ( $T_c$ ) were determined as corresponding to the maximum of the endothermic curve and the minimum of the exothermic curve, respectively. Scanning electron microscopy (SEM) was used to study the morphology of the fracture surface of the specimens via JSM 6100. An X-ray diffraction (XRD) study of the samples was carried out with an M18 X-ray diffractometer (50 kV, 250 mA) with a copper target and nickel filter at a scanning rate of 4°/min. The melt flow index (MFI) was tested with an SRZ-400C MFI Tester (Changchun Mechanical Properties Testing Machine Ltd.) according to Chinese standard GB/T3682-2000 at 260°C.

Samples of the alloy were extracted with toluene for 48 h to remove the PC and SEBS phases, and the remaining PET was dried in a vacuum oven for 72 h at 80°C. Solution viscosity measurements were carried out in a viscosimeter equipped with Ubbelohde capillaries in a mixture of phenol and 1,1,2,2-tetrachloro-

TABLE I  
Mechanical Properties of PET/PC/SEBS Blends by Different Drying Methods

	Tensile strength (MPa)	Elongation at break (%)	Flexural strength (MPa)	Unnotched impact (kJ m <sup>-2</sup> )	Notched impact (kJ m <sup>-2</sup> )
A	48.7	110.9	78.8	NB	17.7
B	47.0	114.2	60.8	NB	14.8
C	45.9	156.0	71.9	NB	12.5
D	45.7	154.3	73.1	NB	13.2

PET and PC were dried at 120°C for 5 h (A), 100°C for 20 h (B), 120°C for 10 h (C), and 100°C for 5 h (D), NB, nonbreak.

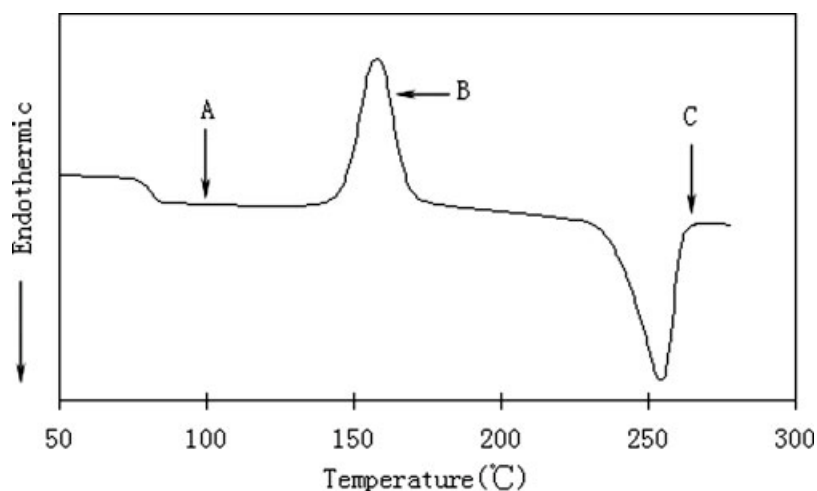


Figure 2 DSC curves for PET scraps.

ethane (60 : 40, v/v) at 25°C. The intrinsic viscosity  $[\eta]$  was determined by a well-known method (extrapolation using the Huggins equation). The weight-average molecular weight ( $M_w$ ) was determined from the Mark-Houwink relation,  $[\eta] = KM_w^\alpha$ . The constants were  $K = 7.44 \times 10^{-4} \text{ dL g}^{-1}$  and  $\alpha = 0.648$  at 25°C.<sup>19</sup>

## RESULTS AND DISCUSSION

### Drying conditions

Seo and Cloyd reported that the drying condition severely affects the properties of PET and the water content in raw PET should be kept at less than 0.02%.<sup>2</sup> PET/PC/SEBS blends were tested under different drying conditions, and the mechanical properties are provided in Table I. The table shows there are no major differences between the results. A higher drying temperature induces the cold crystallization of PET, and a lower drying temperature is not powerful enough to get the drying effect. Because our processing is a low temperature extrusion, the relatively lower drying temperature was adapted here in order to keep the crystallization and orientation structure of the bottle scraps, which were formed in the bottle blowing process. Thus, the drying conditions for our research were chosen as 5–20 h at 100–120°C.

### Effects of extruding temperature

A DSC curve for PET scraps is shown in Figure 2. The extrusion temperature deeply affects the properties of the specimens together with the hydrolysis and thermal degradation of PET. When the extruding temperature is too high, the PET chain is easy to break by hydrolysis and heat degradation and the molecular weight is decreased. Figure 2 shows the  $T_g$  of PET scraps is 81.2°C, the cold  $T_c$  is 151.3°C, and the  $T_m$  is 253.8°C. According to Figure 2, three temperatures

were selected as the extruding temperatures: temperature A is 100°C (between the  $T_g$  and  $T_c$ ), temperature B is 160°C (between  $T_c$  and  $T_m$ ), and temperature C is 260°C (over  $T_m$ ).

Table II shows the mechanical properties of the PET/PC/SEBS alloy extruded at different temperatures. With the rise of the extrusion temperature, the tensile strength of the alloy decreased from 47.00 to 46.01 MPa and the elongation at break decreased from 104% at 100°C to 43% at 160°C and further to 16% at 260°C. The flexural strength and modulus have the same trend, and the notched impact strength has a sharp decrease from 20.36 to 8.55 kJ/m<sup>2</sup>. Table II shows that low temperature extrusion can improve the mechanical properties of the PET/PC/SEBS alloy, because low temperature extrusion can decrease the degradation and hydrolysis of the PET chain and preserve the orientation structure that was preformed by the bottle blowing process. When the alloy was extruded at 160°C, more microcrystals were formed by cold crystallization, which gave rise to phase separation; the mechanical properties were decreased as a result. When the alloy was extruded at 260°C, degradation and hydrolysis of PET chain caused the decrease of the molecular weight of PET and the impact strength was also decreased.

TABLE II  
Mechanical Properties of PET/PC/SEBS Alloy  
Extruded at Different Temperatures

Mechanical property	Extrusion temperature (°C)		
	100	160	260
Tensile strength (MPa)	47.00	44.55	46.01
Elongation at break (%)	103.61	42.59	15.86
Flexural strength (MPa)	70.66	61.97	65.89
Flexural modulus (GPa)	2.15	1.78	1.80
Notched impact strength (kJ/m <sup>2</sup> )	20.36	16.17	8.55

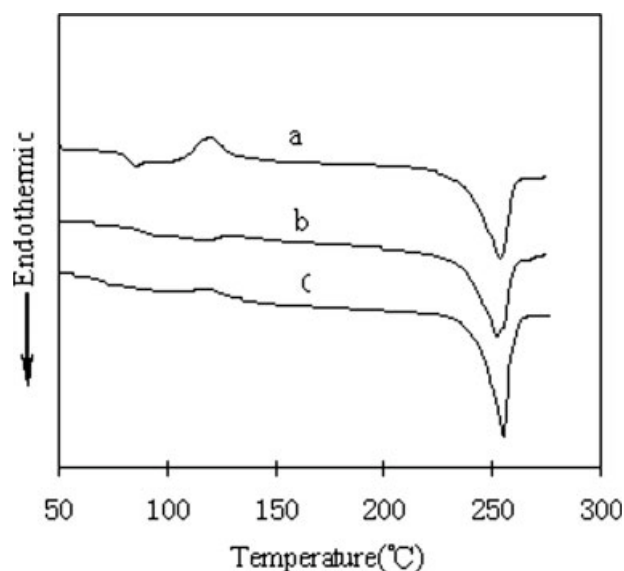


**Figure 3** DSC curves of PET and PET/PC/SEBS alloys extruded at (a) 100, (b) 160, and (c) 260°C.

Figure 3 shows the DSC curves of PET/PC/SEBS alloys. Table III provides the analyzed results of Figure 3. The table shows the crystallinity of PET bottle scraps is 31.7% and the melting temperature is the highest at 257.5°C. The DSC curve for the alloy sample extruded at 100°C shows a big peak for the cold crystal, the  $T_m$  value decreased to 253.7°C, and the crystallinity decreased to 18.6%. The DSC curve for the alloy sample extruded at 160°C has a higher  $T_g$  of 87.9°C and a lower  $T_m$  of 252.8°C together with the highest value for the crystallinity (32.9%). DSC of the alloy samples extruded at 260°C has a  $T_g$  of 71.2°C, a  $T_m$  of 256.0°C, and increased crystallinity of 29.5%. These results are from the following: when the alloy sample was extruded at 100°C, the crystal cells were destroyed by the shear force, the crystallinity was lowered, and the DSC curves showed the cold crystal peak. A temperature of 160°C is up to the  $T_g$  of PET scraps; the lower  $T_m$

**TABLE III**  
Analyzed Results of DSC Curves of PET and PET/PC/SEBS

	$T_g$ (°C)	$T_c$ (°C)	$\Delta H_c$ (J/g)	$T_m$ (°C)	$\Delta H_m$ (J/g)	Crystallinity (wt %)
a	—	—	—	257.50	45.93	31.75
b	81.70	119.20	14.89	253.70	41.78	18.59
c	87.90	—	—	252.80	47.57	32.88
d	71.20	118.30	3.55	256.00	46.28	29.54

- (a) Pure PET scraps.  
(b) Extruded at 100°C.  
(c) Extruded at 160°C.  
(d) Extruded at 260°C.

Crystallinity =  $\frac{\Delta H_m - \Delta H_c}{\Delta H_m^*} \times 100\%$ , where  $\Delta H_m^*$  = 144.664 J/g is the melt enthalpy for 100% crystallized PET and  $\Delta H_c$  is the enthalpy for the cold crystal.

**TABLE IV**  
Intrinsic Viscosity and Weight-Average Molecular Weight of Alloys

	Extrusion temperature (°C)		
	100	160	260
$[\eta]$ (dL/g)	0.68	0.67	0.52
$M_w$ (g/mol)	37,100	36,200	24,500

and the highest crystallinity of the alloy extruded at 160°C results from the breaking of the crystal cells as well as the imperfect crystallization. At the same time, the DSC shows no cold crystal peak during the heating. The alloy sample extruded at 260°C has a higher  $T_m$  and shows the best crystal ability as the melting extrusion process decreased the molecular weight of PET. Table IV gives the  $[\eta]$  and  $M_w$  values. Table V provides the heat distortion temperature (HDT) and the melt flow rate (MFR) of PET/PC/SEBS alloys extruded at different temperatures. The alloy sample extruded at 160°C has the highest heat distortion corresponding to the highest  $T_g$  in Table III. The  $T_g$  in Table III has a corresponding relationship with the HDT shown in Table V. The MFR describes the melt flow ability of thermoplastic polymers. Tables IV and V show that samples extruded at 100 and 160°C had relatively low MFRs and the intrinsic viscosity of PET phases did not decrease much. This is because the low temperature extrusion processing is a process below the  $T_g$ , which can keep the orientation structure of PET scraps and avoid the hydrolysis and degradation of the PET chain. When extruded at 260°C, the MFR of the alloy is higher than 36 g/10 min, which is because the molecular weight is decreased and the distribution of the molecular weight is wider, which results in the decrease of the viscosity of the polymer melt.

The PET/PC blends without compatibilizer possess poor mechanical properties.<sup>20–28</sup> Therefore, it is necessary to compatibilize these blends. Previous work demonstrated that the compatibility and adhesion can be improved by the addition of suitable copolymers, which act as compatibilizers located at the interface between immiscible phases. PET/PC/SEBS alloys have a multiphase structure as shown in Figure 4. Figure 4 presents the SEM images for the impact broken surfaces of PET/PC/SEBS alloys extruded at different tem-

**TABLE V**  
Heat Distortion Temperatures and Melt Flow Rates of PET/PC/SEBS Alloys Extruded at Different Temperatures

	Extrusion temperature (°C)		
	100	160	260
HDT (°C)	93	97	94
MFR (g/10 min)	13	9	36

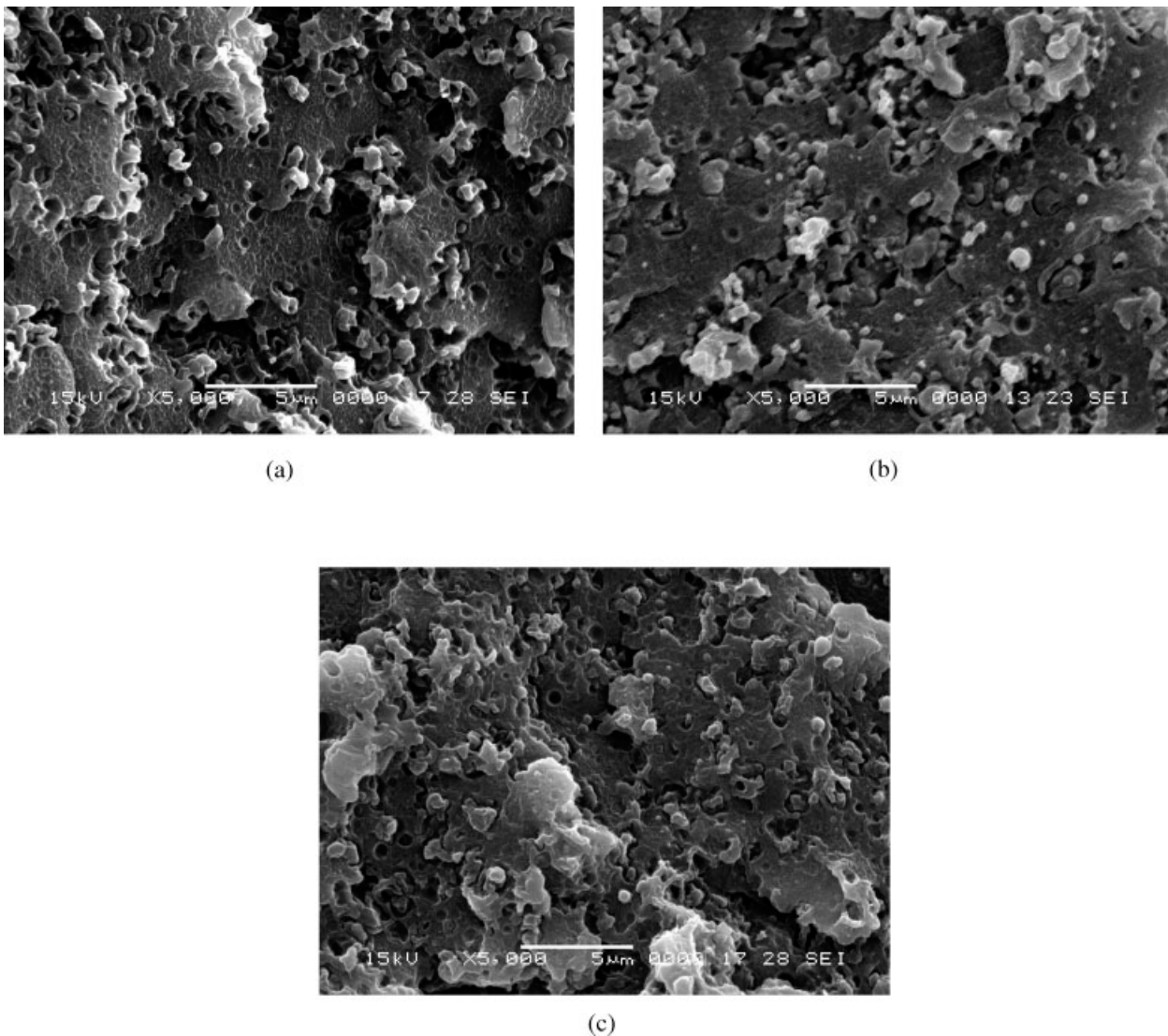


**Figure 4** SEM images (original magnification  $\times 5000$ ) for PET/PC/SEBS alloys extruded at (a) 100, (b) 160, and (c) 260°C.

peratures. The particles of PC are dispersed in the PET matrix, and SEBS acts as the compatibilizer.

#### Effect of extruding speed

The rotation speed of the screws and the blending time of the alloy can both affect the shear force. Table VI shows the effects of the rotation speed of the screws on the mechanical properties of PET/PC/SEBS.

The mechanical properties increased with the rotation speed of the screws and then decreased when the rotation speed was over 150 rpm. The tensile strength was increased 14.7% and the elongation at break was increased 4 times when the rotation speed changed from 50 to 100 rpm. The best properties were attained when the rotation speed of the screws was 100 rpm. When the rotation speed of the screws was relatively lower, such as 50 rpm, the shear power was relatively less, the PC domain in the PET matrix was larger, and

the mechanical properties were not improved significantly. The shear power increased when the rotation speed was up to 100 rpm. The dispersion of the PC phase in PET was fine and the properties were improved. As the rotation speed of the screws increased

**TABLE VI**  
Effects of Rotation Speed of Screws on Mechanical Properties of PET/PC/SEBS Alloys

	Rotation speed (rpm)			
	50	100	150	200
Tensile strength (MPa)	40.96	46.98	45.90	46.57
Elongation at break (%)	26.53	135.67	156.03	113.78
Flexural strength (MPa)	72.26	76.38	71.94	78.45
Flexural modulus (GPa)	2.16	2.31	2.11	2.33
Unnotched impact strength ( $\text{kJ/m}^2$ )	29.23	NB	NB	59.38
Notched impact strength ( $\text{kJ/m}^2$ )	9.62	15.74	12.50	9.18

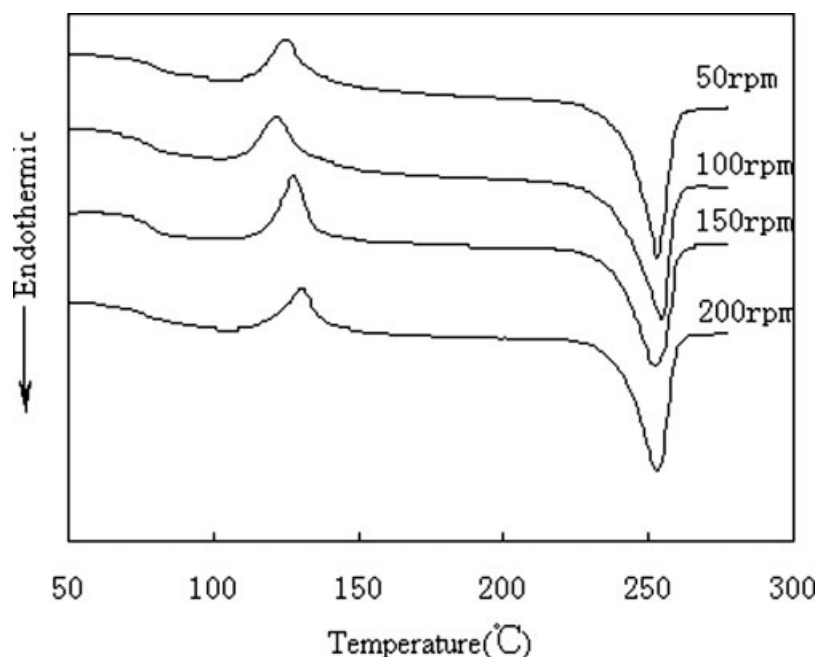


Figure 5 DSC curves of PET/PC/SEBS alloys extruded at different screw speeds.

TABLE VII  
DSC Results of PET/PC/SEBS Alloy Extruded at Different Screw Speeds

Screw speed (rpm)	$T_g$ (°C)	$T_c$ (°C)	$\Delta H_c$ (J/g)	$T_m$ (°C)	$\Delta H_m$ (J/g)	Crystallinity (wt %)
50	79.50	125.00	14.24	253.00	40.82	18.37
100	77.50	121.70	15.94	254.70	41.08	17.37
150	78.30	127.70	17.28	252.30	40.54	16.08
200	75.60	130.40	13.46	252.90	40.82	18.91

to 150–200 rpm, the viscosity of PET was decreased by the overload shear power, the phase domain was large, and the properties of the alloy were lower. Relative to 150 rpm, the properties of the alloy extruded at 200 rpm were decreased severely as the PC domain in the PET matrix became larger.

Figure 5 and Table VII contain the DSC curves of PET/PC/SEBS alloys extruded at different screw rotation speeds. The rotation speed of the screws was increased; when the rotation speed was suitable, the blend alloy had an appropriate viscosity and the crystal grain could be broken by shear force, which decreased the crystallinity. The decrease of the crystallinity simultaneously caused the lowering of the  $T_g$  and  $T_c$ .

Table VIII shows the MFRs of PET/PC/SEBS alloys extruded at different screw speeds. The table shows the MFRs decreased with the rise of the screw rotation speed, which indicates the shear power induced the structure variety of PET/PC blends. The shear power accelerated the dispersion of both PC and SEBS phases together with improving the orientation of PET, which was advantageous to the formation of the network and the minisandwich structure. The structure of the blend

system became more complex and the MFR decreased with the increase of the rotation speed of the screws.

Figure 6 provides SEM images of the impact broken surfaces of samples extruded at different screw rotation speeds. Samples were etched in chloroform, and PC and SEBS were dissolved. Figure 6(a) shows there is only deformation and orientation of the PC phase, and the morphology of the PC phase is shown as big particles. These particles are fine and become smaller in Figure 6(b) with an average diameter of 1  $\mu\text{m}$ . The separation phase becomes much bigger in Figure 6(c,d). When the speed was 100 rpm, the SEBS and PC phases dispersed in PET in a suitable way; both the PET phase and the separate phase could form the continued network and the properties of the blends were greatly improved. When the rotation speed was too

TABLE VIII  
Melt Flow Rate of PET/PC/SEBS Alloy Extruded at Different Screw Speeds

	Screw speed (rpm)			
	50	100	150	200
MFR (g/10 min)	14.1	10.1	9.2	9.0

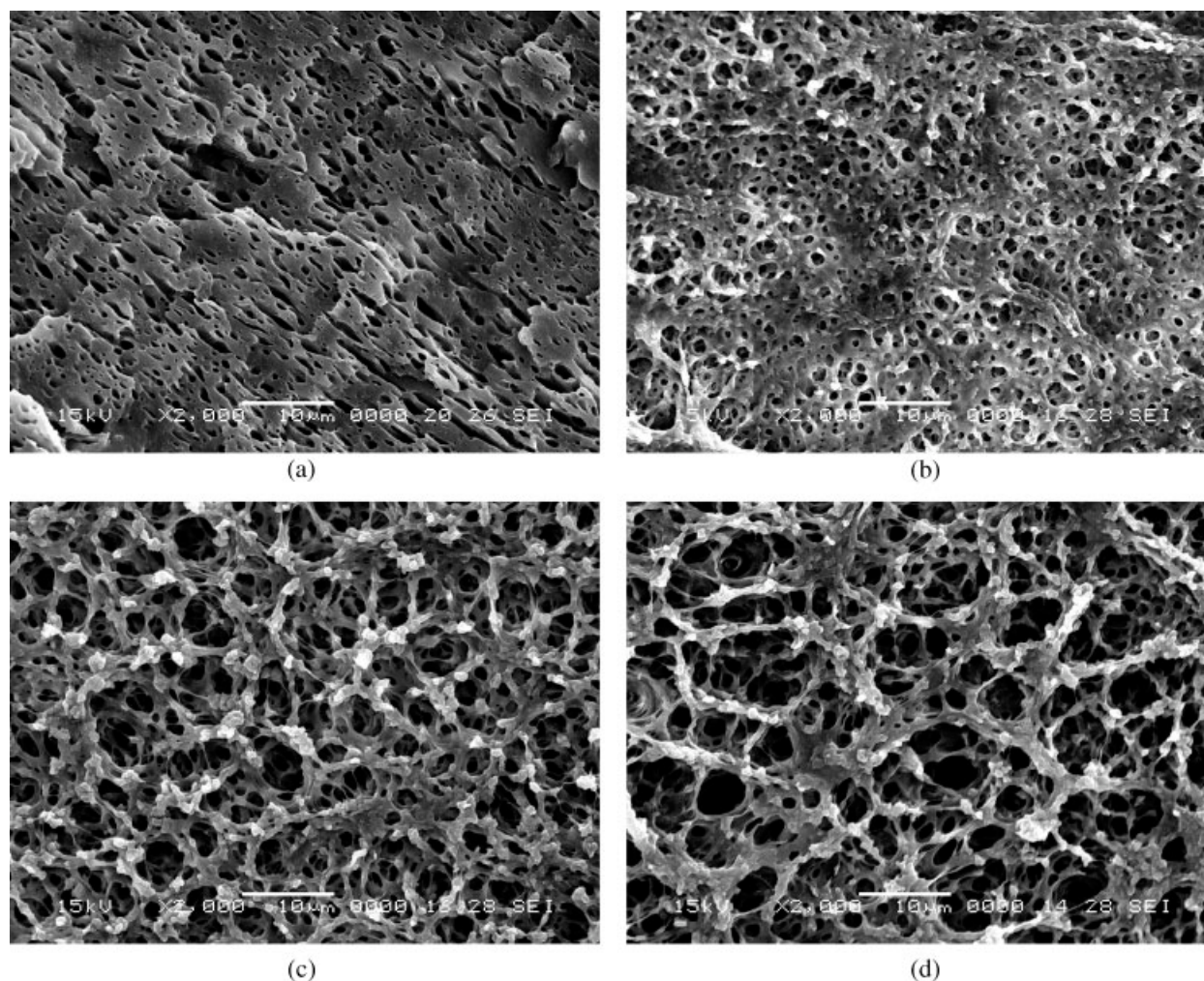


**Figure 6** SEM images (original magnification  $\times 2000$ ) of the impact broken surfaces of PET/PC/SEBS samples (etched by chloroform) extruded at screw rotation speeds of (a) 50, (b) 100, (c) 150, and (d) 200 rpm.

fast, the viscosity of PET decreased and the difference in the viscosity of the PET and PC phase became obvious; although the network was formed, the separate phase was oversized and the mechanical properties decreased. The best properties (such as mechanical properties and temperature resistance) could be reached under suitable extrusion processing conditions such as 100 rpm.

### CONCLUSION

Low temperature solid-state extrusion is a novel processing technology.<sup>29–37</sup> Via this processing method, the properties of PET/PC/SEBS alloys can be greatly improved, especially the notched impact strength of the polymer alloy. Low temperature solid-state extrusion limited hydrolysis and thermal degradation of PET because the extrusion temperature was between the glass-transition and cold-crystallization temperatures of PET. The optimized extrusion temperature was 100°C with a rotation speed of 100 rpm. Modifica-

tion of recycled PET by low temperature solid-state extrusion is an interesting method; it not only provides an easy method to recycle PET scraps by blend processing, but it can also form novel structures such as orientation, crystallization, and the network in the alloy. This processing technology also shows a potential way to avoid degradation during processing in polymer blends such as natural fiber filled polymer alloys.

This work was supported by the Natural Science Foundation of China.

### References

- Selke, S. E. *Plastics Recycling*; McGraw-Hill: New York, 2002; p 693.
- Seo, K. S.; Cloyd, J. D. *J Appl Polym Sci* 1991, 42, 845.
- Kalfoglou, N. K.; Skafidas, D. S.; Kallitsis, J. K.; Ambert, J. C.; Stapper, L. V. *Polymer* 1995, 36, 4453.
- Kim, D. H.; Park, K. Y.; Suh, K. D. *J Appl Polym Sci* 2000, 78, 1017.
- Torres, N.; Robin, J. J.; Boutevin, B. *J Appl Polym Sci* 2001, 81, 2377.

6. Dimitrova, T. L.; La Mantia, F. P.; Pilati, F.; Toselli, M.; Valenza, A.; Visco, A. *Polymer* 2000, 41, 4817.
7. Papadopoulou, C. P.; Kalfoglou, N. K. *Polymer* 2000, 41, 2543.
8. Champagene, M. F.; Huneault, M. A.; Roux, C. *Polym Eng Sci* 1999, 39, 976.
9. Yoon, W. H.; Lee, H. W.; Park, O. O. *J Appl Polym Sci* 1998, 70, 389.
10. Papke, N.; Karger-Kocsis, J. *Polymer* 2001, 42, 1109.
11. Wayne, D. C. *J Appl Polym Sci* 1996, 62, 1709.
12. Bong, S. K.; Roger, S. P. *Macromolecules* 1985, 18, 1214.
13. Donald, J. M.; Roger, S. P. *Macromolecules* 1985, 18, 1218.
14. Daisuke, S.; Kazuyo, T.; Toshiyuki, I.; Koh, N. *J Polym Sci Part B: Polym Phys* 2002, 40, 95.
15. Daisuke, S.; Kazuyo, T.; Aki, S.; Tetsuo, K. *Macromolecules* 2003, 36, 3601.
16. Nesarikar, A. R.; Carr, S. H.; Khait, K. *J Appl Polym Sci* 1997, 63, 1179.
17. Ju, M. Y.; Chang, F. C. *Polymer* 2000, 41, 1719.
18. Zeng, B.; Liu, Q.; Zhang, M. *Polymer Materials Science and Engineering* 1991, 7, 110.
19. Berkowitz, S. *J Polym Sci* 1984, 29, 4353.
20. Park, J. G.; Kim, D. H.; Suh, K. D. *J Appl Polym Sci* 2000, 78, 2227.
21. Sanchez-Solis, A.; Estrada, M. R.; Cruz, M. J. *Adv Polym Technol* 2000, 19, 34.
22. Tanrattanakul, V.; Hiltner, A.; Baer, E. *Polymer* 1997, 38, 2191.
23. Tanrattanakul, V.; Hiltner, A.; Baer, E. *Polymer* 1997, 38, 4117.
24. Tanrattanakul, V.; Perkins, W. G.; Massey, F. L.; Moet, A.; Hiltner, A.; Baer, E. *J Mater Sci* 1997, 32, 4749.
25. Vladimir, N. I. *Polymer* 1997, 38, 195.
26. Garcia, M.; Eguiaza, B.; Naza, B. J. *J Appl Polym Sci* 2001, 81, 121.
27. Kong, Y.; Hay, J. N. *Polymer* 2002, 43, 1805.
28. Regina, J. *Macromol Symp* 2000, 170, 21.
29. Lu, X. F.; Hay, J. N. *Polymer* 2001, 42, 9423.
30. Wang, Z. G.; Hsiao, B. S.; Sauer, B. B.; Kampert, W. G. *Polymer* 1999, 40, 4615.
31. Paola, M.; Annamaria, C.; Maurizio, F.; Marina, G. *Eur Polym J* 2003, 39, 1081.
32. Hiroyuki, K. *Appl Polym Sci* 1994, 53, 527.
33. Maurizio, F. *Polymer* 1997, 38, 413.
34. Vladimir, N. I. *Polymer* 1997, 38, 201.
35. Ma, D. Z.; Zhang, G.; He, Y.; Ma, J.; Luo, X. *J Polym Sci Part B: Polym Phys* 1999, 37, 2960.
36. Zhang, G.; Ma, J.; Cui, B.; Luo, X.; Ma, D. *Macromol Chem Phys* 2001, 202, 604.
37. Garcia, M. *J Appl Polym Sci* 2001, 81, 121.